

A COMPARATIVE STUDY OF DIGITAL ROCK PHYSICS AND LABORATORY SCAL EVALUATIONS OF CARBONATE CORES

A. Grader (Ingrain, Inc.), M.Z. Kalam (ADCO), J. Toelke, Y. Mu, N. Derzhi, C. Baldwin, M. Armbruster (Ingrain, Inc), T. Al Dayyani, A. Clark, G. Bin-Dhaaer Al Yafei, B. Stenger (ADCO, Abu Dhabi Company for Onshore Operations)

This paper was prepared for presentation at the International Symposium of the Society of Core Analysts held in Halifax, Nova Scotia, Canada, 4-7 October, 2010

ABSTRACT

A pilot study was recently undertaken in order to evaluate a number of reservoir characterization and petrophysical parameters using Digital Rock Physics (DRP). The chosen core samples were part of a prolific, but mature oil producing carbonate reservoir, on-shore Abu Dhabi. A highly focused set of special core analysis (SCAL) data were acquired earlier on the core samples comprising different reservoir rock types of varying levels of heterogeneity, lithology, porosity, and absolute permeability. This set of measurements formed the baseline for our comparison study. Several of these reservoir core samples were then used in the DRP study to evaluate water-oil relative permeabilities, capillary pressures, Archie cementation exponents 'm', saturation exponents 'n', and elastic parameters such as compressional/shear wave velocities.

The current paper presents a comparison between rock property evaluations from laboratory tests, which took over two years to complete, and the Digital Rock Physics study, which required only three months.

The comparison demonstrated an overall satisfactory match between data obtained by DRP and laboratory tests. It was therefore concluded, that Digital Rock Physics has the potential to significantly improve the quality and timeliness of reservoir characterization studies because of the quick turnaround time characteristic for DRP studies and the quality of data it provides.

INTRODUCTION

Digital Rock Physics (DRP) is a novel way of investigating and estimating the physical and fluid flow properties of porous rocks. In this approach, high-resolution images of the rock's pores and mineral grains are obtained and processed, and the rock properties are evaluated by numerical simulation of the physical processes of interest at the pore scale.

Comparisons between the rock properties obtained by DRP studies and those obtained by other means (laboratory SCAL tests, wireline logs, well tests, etc.) are important to validate this new technology and use the results it provides with confidence. In this paper

we present a comparative study of DRP and laboratory SCAL evaluations of carbonate cores. To the best of our knowledge, this is the first published study of its kind.

MATERIALS AND METHODS

Characterization of the Reservoir Core Samples

The study was conducted on eight 1½" diameter cylindrical core plugs representing four Lower Cretaceous carbonate reservoir rock types ("RRT"), according to a current Abu Dhabi Company for Onshore Operations (ADCO) RRT definition [1]. This ADCO definition is based mainly on the sample's porosity, permeability and mercury injection capillary pressure measurements. This characterization had also been linked to a standardized ADCO lithofacies description, and assumed environment of deposition [2]. Because two of these rock types (RRT-3 and RRT-4) are similar in many properties, in this paper we cover results from only six core plugs, which cover a selection of three contrasting rock types: RRT-2, RRT-4 and RRT-6.

These three RRTs are each described below, using some of the plugs for illustrative purposes.

RRT-2:

Sample S18 is an example of Coated-Grain, Algal, Skeletal Rudstone to Floatstone "CgASR" lithofacies, from a depth of 8247.17 ft (MD). The measured NMR porosity for this plug is 29.7%, and the gas permeability is 240 mD, implying this sample belongs to "RRT 2", according to the previously mentioned ADCO scheme. The "CgASR" lithofacies implies deposition in a shallow subtidal, high-energy open platform above fair weather wave base, upper ramp, near shoal crest. Typical thin section and MICP curves for rock type 2 are presented in Figures 1 and 2.

RRT-4:

Sample 22 is an example of Skeletal, Peloid Packstone (SPP) lithofacies, from a depth of 8029.00 ft (MD). The measured NMR porosity for this plug is 35.2%, and the permeability (water) is 21.8 mD, implying this sample belongs to "RRT 4". The SPP lithofacies implies deposition in shallow subtidal to intertidal, moderate-energy restricted and open platform above fair weather wave base, possibly, inner shoal and upper ramp. Typical thin section and MICP curves for rock type 4 are presented in Figures 3 and 4.

RRT-6:

Sample 33 is an example of Orbitolinid, Skeletal Wackestone (OSW) lithofacies, from a depth of 8159.25 ft (MD). The measured NMR porosity for this plug is 24.3%, and the permeability (water) is only 0.82 mD, implying this sample belongs to "RRT 6". The OSW lithofacies implies deposition in low-energy, open platform below fair weather wave base, possible middle ramp. Typical thin section and MICP curves for rock type 6 are presented in Figures 5 and 6.

Laboratory Tests

The laboratory test data used in this study were accumulated by ADCO in the course of several years. The tests were performed on cores from the same rock type and formation, but not necessarily on the same cores used in this DRP study. A number of commercial and research laboratories were involved in testing, and they used a variety of methods for SCAL: centrifuge, porous plate, steady-state, unsteady-state, and others.

Laboratory SCAL studies, especially those involving steady-state and porous plate methods, may take over two years to complete.

Digital Rock Physics (DRP) Methods

For the purposes of this study, the images of the rock samples' structure were obtained utilizing X-Ray Computed Tomography (CT) with resolutions ranging from 100 nanometers to 40 micro-meters. The images were processed (segmented) to identify locations in the rock occupied by various minerals and pores. The result of this process is a digital rock, i.e. a 3-D matrix of the same size as the CT image, where each cell is either a solid, or a pore, and is assigned elastic properties and conductivity accordingly to the mineral or fluid occupying the corresponding location in the rock sample.

We used the lattice Boltzmann method (LBM) to simulate the laminar flow of single or multiple fluids through the digital rock [3]. The 3-D pore structure defined by three-dimensional high-resolution CT imaging forms the grid system for using the LBM method to compute fluid transport properties: absolute permeabilities, relative permeabilities, and capillary pressures. The capillary pressure simulations also provide fluid (*e.g.*, oil/water) distributions throughout the digital rock, which are then used to assign conductivities to the pore cells in the course of estimating the resistivity index and determinations of Archie's saturation exponent 'n'. The computational parameters (including fluid viscosities, interfacial tensions, and contact angles) were selected to match the experimental conditions in the laboratory tests. Experimental constraints such as fluid flow velocities and aging were also considered in determining two-phase oil-water relative permeabilities.

The elastic properties of the rocks were estimated from simulating elastic deformations in the digital rock. The rock's conductivity and related formation resistivity factor, resistivity index, cementation and saturation exponents ('m' and 'n' respectively) were estimated from numerical simulation of the electric current in the rock.

RESULTS AND DISCUSSION

Basic Core Properties

The graph presented in Figure 7 summarizes the porosity-permeability results obtained by DRP and their comparison with the values obtained from laboratory tests. The RRT4 (orange) and RRT 6 (purple) are mainly uni-modal structure and they form an almost continuous trend. The blue points represent RRT2 that has a bi-modal structure, and has relatively higher permeabilities than the other rock types. The total porosity of the samples included porosity that can be directly defined by the CT data and micro-porosity

in the micro-crystalline (MC) phase. The porosity in the MC phase was determined either by nano-CT imaging or by linear phase segmentation of the micro-CT data. The typical contributions of micro-porosity to the total porosity were (in decimal fractions) 0.5-0.6, 0.6-0.7, and 0.7-0.9 for RRT 2, 4, and 6, respectively. The determination of the micro-porosity phase and its properties plays a significant role in determining the elastic properties and the formation factor/resistivity index.

Electrical Properties

The graph presented in Figure 8 summarizes the formation resistivity factor results obtained by DRP and their comparison with the values obtained from laboratory tests. The DRP data form a continuous trend that merges well with laboratory data. The laboratory data are not all for the same samples used in the DRP studies. In some lab tests resistivity factors were not measured. The graph presented in Figure 9 summarizes the resistivity index results obtained by DRP and their comparison with the values obtained from laboratory tests. There is a reasonable match between the lab data and DRP data. Moreover, the trend for the micritic samples of RRT 6 show a good match even along the changing “n” value (related to the slope of the curve through the data) at lower saturation. Tables 1 and 2 present the comparison of the DRP and physical laboratory results for Archie’s cementation exponent ‘m’, and Archie’s saturation exponent ‘n’, respectively. The poor match of ‘n’ for RRT 6 is probably driven by the micritic nature of the sample and was under further investigation at the time of writing.

The cementation exponent ‘m’ was computed by obtaining the formation factor and the porosity of several digital rock samples from the same plug, as shown in Figure 8. The effect of the saturated micro porosity on the formation factor was taken into account by assigning a specific conductivity to the micro-porous phase based on either direct DRP computations on the samples in the study or by using comparable DRP data from other samples from similar Middle East carbonates. The saturation (drainage) exponent ‘n’ was determined by computing the formation factor for several saturation maps obtained during the primary drainage capillary pressure DRP simulation and generating diagrams similar to Figure 9. Only saturation maps in which the oil has arrived at the outlet end of the sample were used in the computation of ‘n’. In the case of a bi-modal structure, such as in RRT 2, the combined drainage Pc data (micro and macro porosities) were used.

Table 1. Cementation exponent values

"m"	Rock Type	Lab min	Lab max	DRP average
	RRT2	1.96	2.21	1.99
	RRT4	1.89	2.07	1.75
	RRT6	1.77	2.15	2.01

Table 2. Saturation exponent values

"n"	Rock Type	Lab min	Lab max	DRP average
	RRT2	1.88	2.09	1.95
	RRT4	1.87	1.98	2.1
	RRT6	1.54	1.75	2.74

Elastic Properties

No laboratory tests of compressional (V_p) and shear (V_s) velocities were performed on the cores included in this study. For comparisons (illustrated in Figures 10 and 11), we used the values obtained from laboratory tests on cores from the same and adjacent wells, as well as values from a published study [4] of velocities in carbonate outcrops (green triangles and diamonds). The velocity values provided by DRP agree well, in general, with those obtained in the laboratory tests done at reservoir condition. The dynamic elastic moduli (e.g. Young's modulus shown in figure 11) calculated from these velocities are also in good agreement with the data from the lab.

Imbibition Relative Permeability

The comparisons of relative permeability values obtained by DRP and by physical laboratory tests are presented in Figures 12 (RRT 2) and 13 (RRT 4). In all cases, relative permeabilities were scaled by K_{ro} at Sw_{irr} and all DRP derived relative permeabilities were computed at imbibition steady-state conditions. For the sake of brevity, not all the comparisons done for this study are shown. Figure 12(a) shows a semi-log plot of DRP K_r (open diamonds) and laboratory K_r (solid diamonds). The DRP curves are derived from core S9 (RRT 2). The laboratory data are from a composite core from the same rock type. The match between the curves and the residual saturations is satisfactory. Two more K_r curves are added in Figure 12(b). One of them (denoted by triangles) represents a steady-state laboratory experiment from another RRT 2 core. The second set of curves (denoted by solid circles) was generated by the unsteady-state method coupled with imbibitions capillary pressure measurements (centrifuge and semi-dynamic method), but were deemed unrealistic.

Figure 13(a) shows a semi-log plot of DRP K_r (open diamonds) and laboratory K_r (solid diamonds). The DRP K_r values were computed on the same sample that was used in the lab (sample 22 RRT 4). In Figure 13(b) a third set of K_r curves (unsteady-state method) is added denoted by solid circles. The water relative permeability is similar to the first two curves. The oil relative permeability curve is significantly lower than the first two curves.

Drainage Capillary Pressure

Figures 14 (RRT 2) and 15 (RRT 4) present DRP (open symbols) and laboratory (solid symbols) primary drainage capillary pressure curves. All the DRP curves simulated porous plate experiments. In Figure 14, the capillary pressure is controlled by macro porosity. Two DRP results from different sub-samples in the core plug are shown exhibiting similar results. The residual water saturation is between 8% and 12%. The laboratory results are on the same rock type but different core plugs. All the laboratory results approach a similar range of residual water saturation. Figure 15 (for RRT 4) shows two DRP curves. The uppermost curve (open diamonds) is from a tight portion of the sample and exhibits a drainage "bench" at a pressure of about 2 bars. It represents a small fraction of the rock bulk volume and can be added to the low capillary pressure curve denoted by the open circle. There are five laboratory-derived capillary pressure

curves for the same rock type. Four of them match the DRP curve (open circles) quite well. The laboratory curve on the lower left (solid diamonds) represents multi-speed centrifuge data.

CONCLUSION

The validation study presented in this paper is the extensive investigation of DRP involving carbonate reservoir rock types. It demonstrated that DRP has significant potential to provide quality data in a short time frame. DRP opens a new possibility to quickly investigate the sensitivity of rock properties to variations in experimental conditions.

ACKNOWLEDGEMENTS

The authors acknowledge the support of Ingrain, Inc and Abu Dhabi Company for Onshore Operations (ADCO) in conducting this study. The authors acknowledge ADCO and ADNOC management for permission to publish the results of this study.

REFERENCES

1. Grötsch, J. (June 1997): Reservoir Rock Type Scheme for the Upper Thamama Reservoirs: A Basis for the Integrated 3-D Reservoir Characterization Study, *Internal ADCO Report*.
2. Strohmenger, C. J., L. J. Weber, A. Ghani, K. Al-Mehsin, O. Al-Jeelani, A. Al-Mansoori, T. Al-Dayyani, L. Vaughan, S. A. Khan, and J. C. Mitchell. *Giant Hydrocarbon Reservoirs of the World: From Rocks to Reservoir Characterization and Modeling* AAPG Special Publication Memoir 88 (2006), 139-171.
3. Toelke, J., C. Baldwin, Y. Mu, N. Derzhi, Q. Fang, A. Grader, J. Dvorkin “Computer simulations of fluid flow in sediment: From images to permeability” *The Leading Edge*, (2008) **27**, 1040-1048.
4. Vanorio, T., C. Scotellaro, and G. Mavko “The effect of chemical and physical processes on the acoustic properties of carbonate rocks” *The Leading Edge*, (2010) **29**, 68-74.

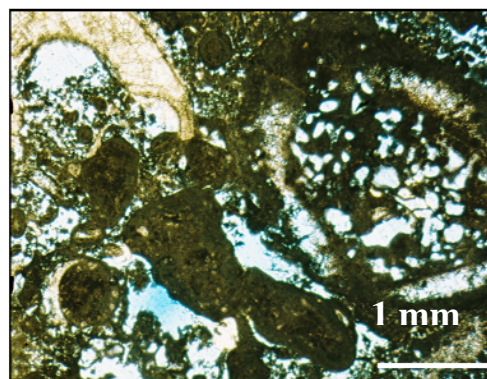


Figure 1. Typical thin-section of CgASR lithofacies. Porosity is indicated by bluish colour. Sample porosity is about 22%.

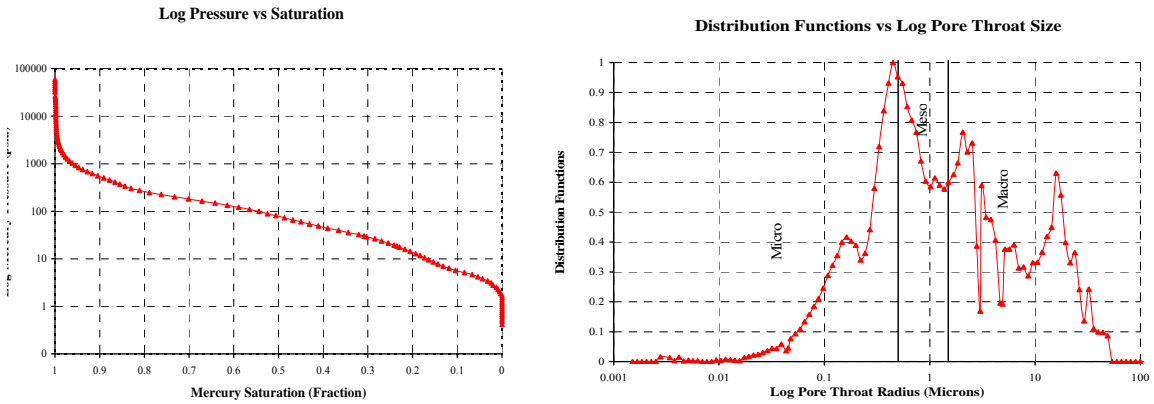


Figure 2. MICP results for Sample S18, RRT 2, bi-modal.

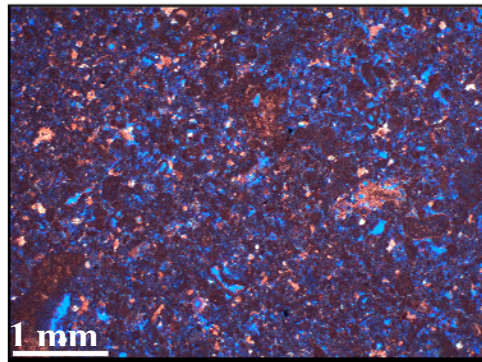


Figure 3. Typical thin-section of SPP lithofacies. Porosity is indicated by blue colour. Sample porosity is about 35%.

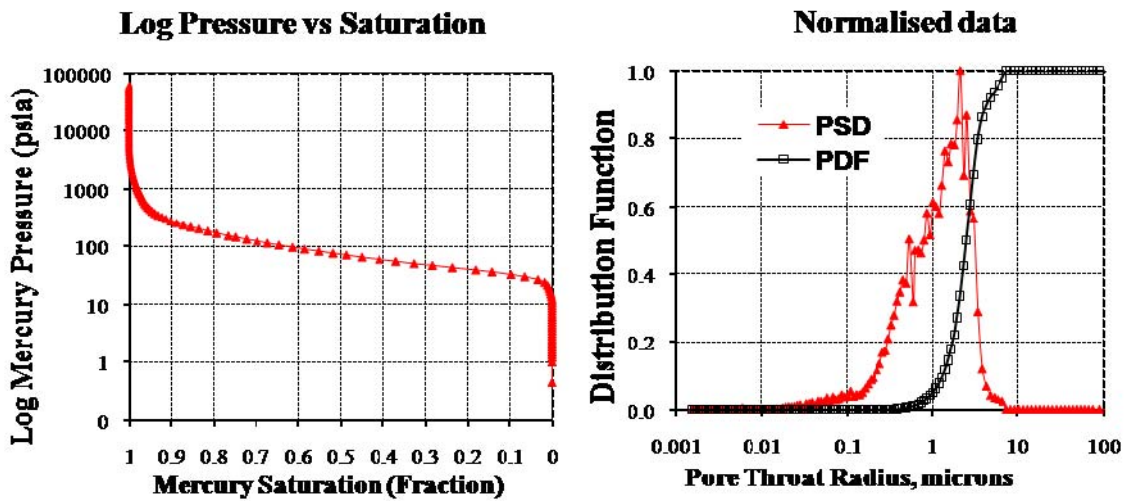


Figure 4. MICP results for Sample 22, RRT 4 uni-modal structure.

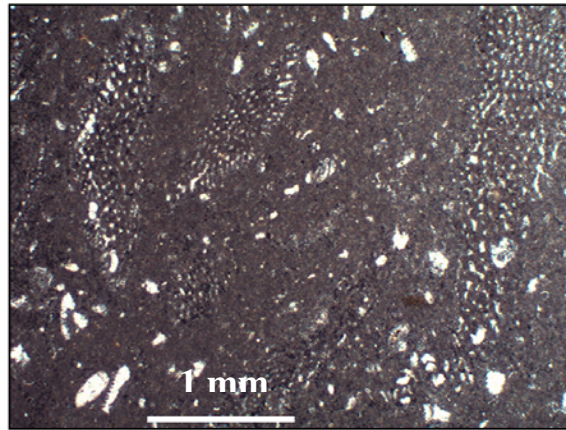


Figure 5. Typical thin-section of OSW lithofacies. Porosity is indicated by blue colour. Sample porosity is about 24%.

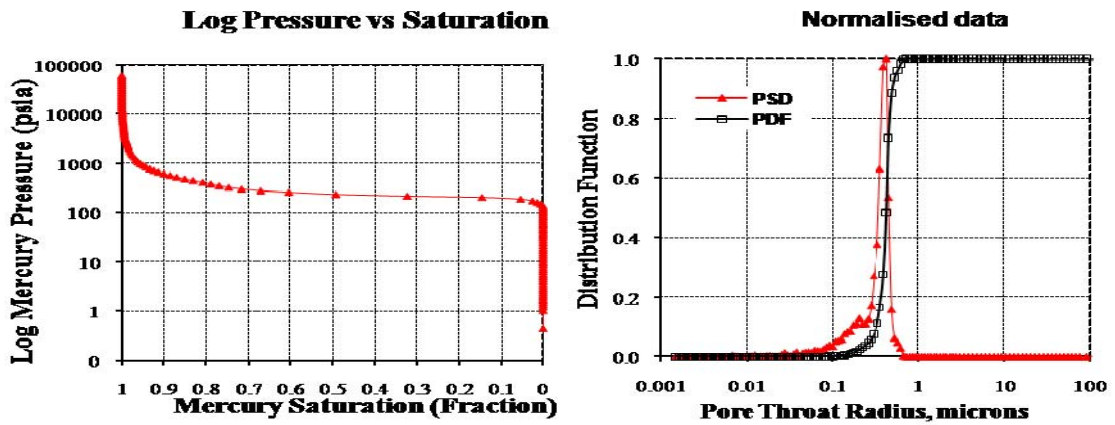


Figure 6. MICP results for Sample 33, RRT 6, uni-modal structure.

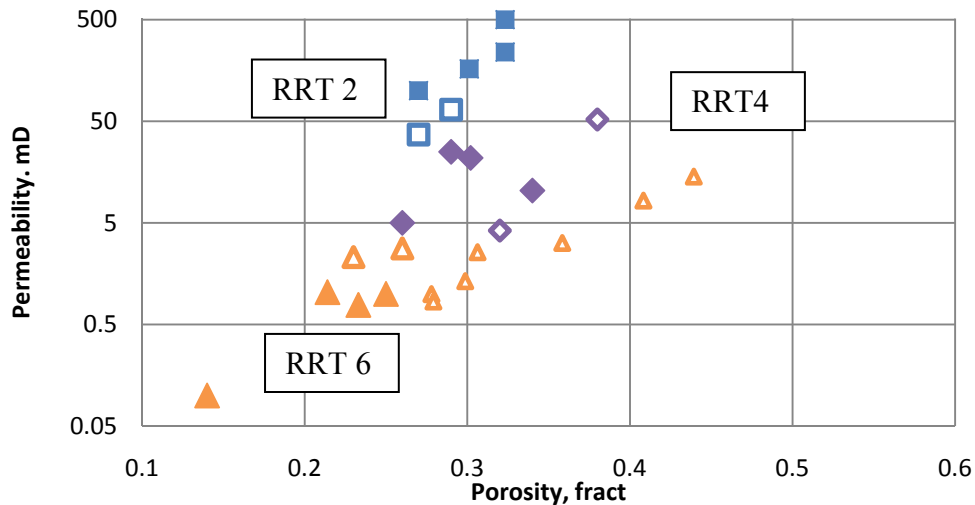


Figure 7. Permeability-positivity trends resulting from laboratory tests (solid diamonds) and DRP (open circles). Small open circles display permeability-positivity trend for RRT6, obtained by sub-sampling the digital rocks. Different colours identify rock types.

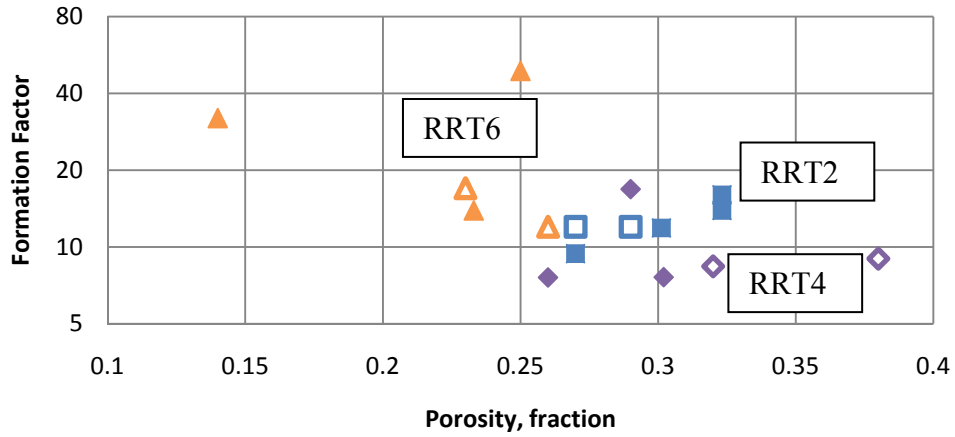


Figure 8. Formation resistivity factor-porosity trends resulting from laboratory tests (solid diamonds) and DRP (open circles). Different colours identify rock types.

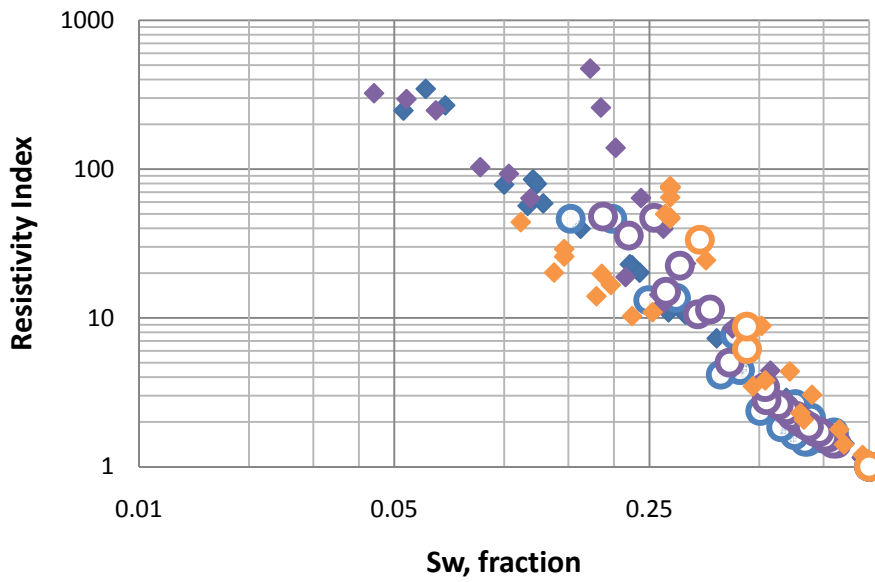


Figure 9. Resistivity index-water saturation trends resulting from laboratory tests (solid diamonds) and DRP (open circles). Different colours identify rock types.

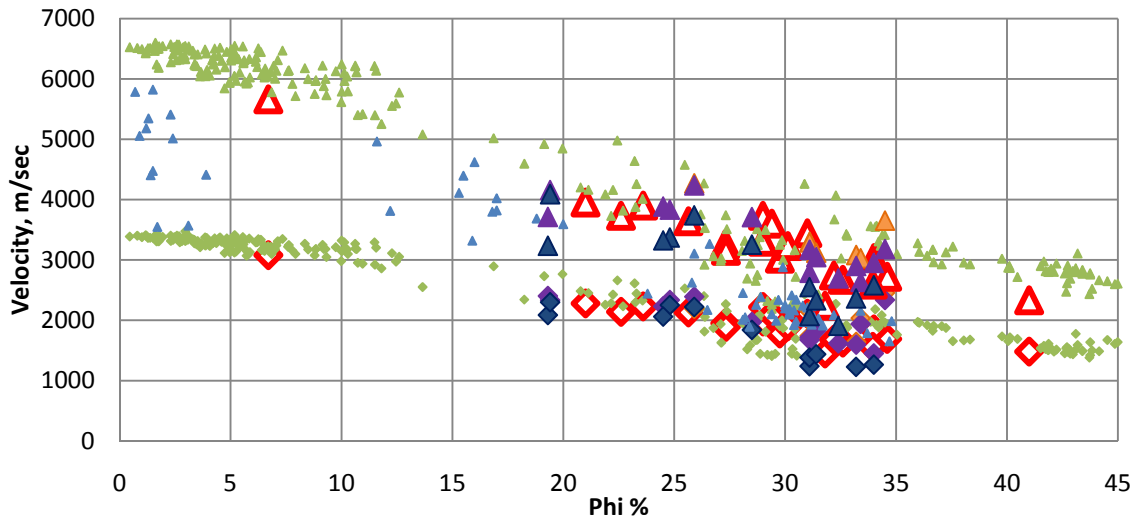


Figure 10. Pressure and shear velocity-porosity trends. Diamond symbols represent V_s values, triangles – V_p . Open symbols represent DRP results, solid symbols – laboratory tests at different effective stress conditions (ambient, 7 MPa, 30 MPa, 44 MPa). The small green triangles are data that were collected for carbonate outcrops.

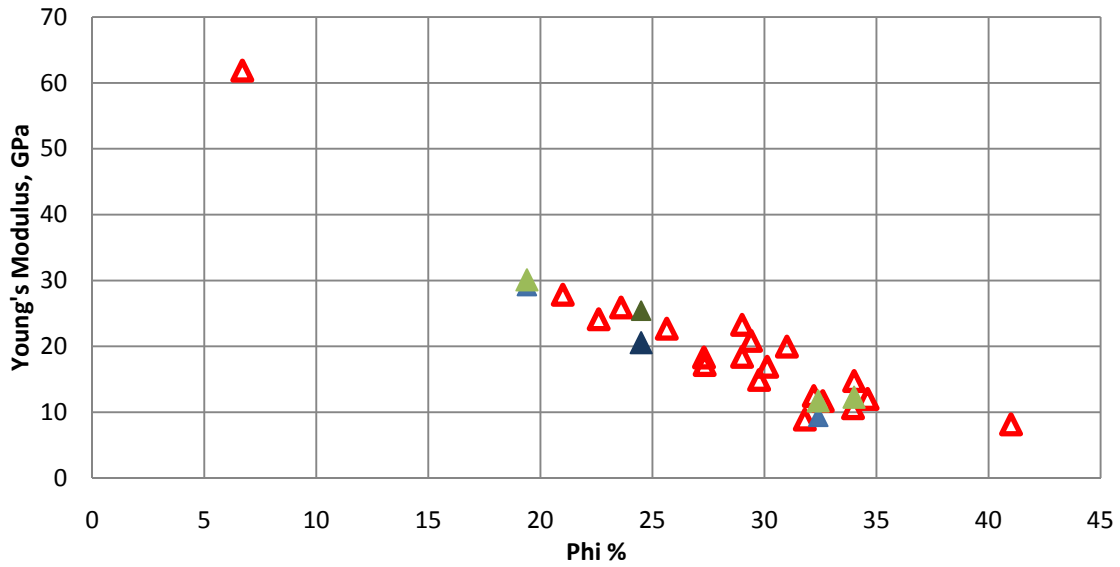


Figure 11. Young's modulus-porosity trend. Open symbols represent DRP results, solid symbols - laboratory tests at different effective stress conditions.

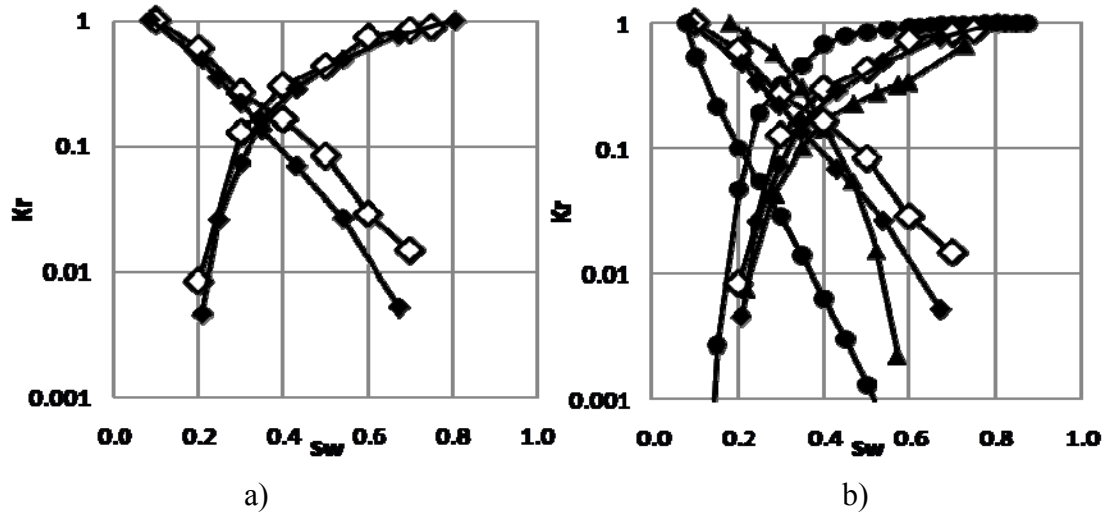


Figure 12. Semi-log plot of relative permeability curves for Rock Type 2, sample S9. Open diamonds – DRP results, solid diamonds – steady-state laboratory test on a composite core from rock type 2. Other laboratory test data are added in plot b): unsteady-state method (circles) and steady-state method on another core of rock type 2 (triangles)

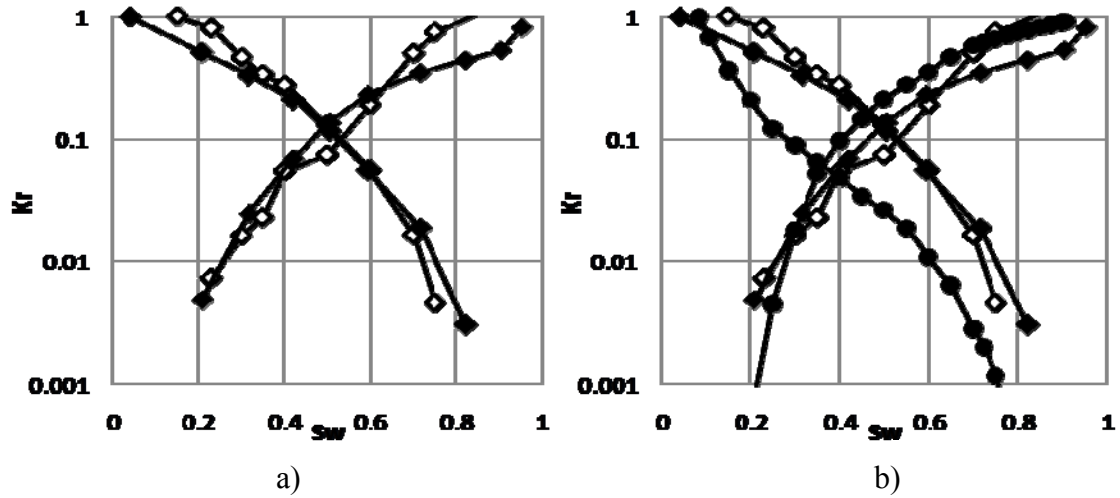


Figure 13. Semi-log plot of relative permeability curves for Rock Type 4, sample 22. Open diamonds – DRP results, solid diamonds – steady-state laboratory test on the same core (a). Other laboratory test data obtained in unsteady-state test (circles) are added in plot (b).

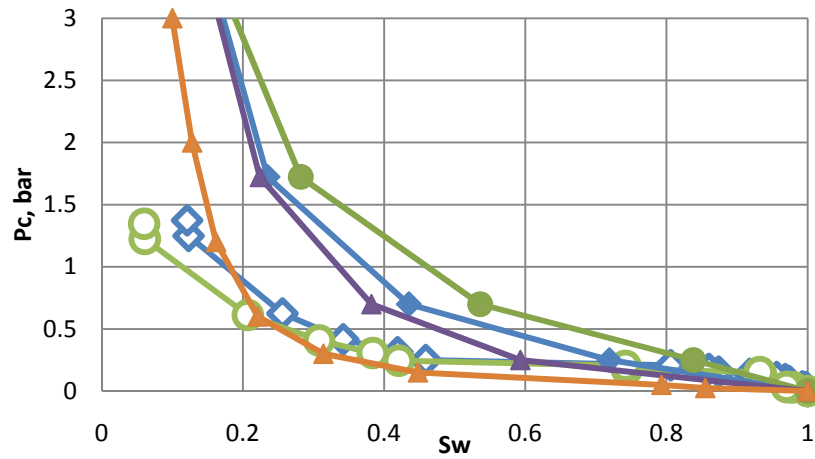


Figure 14. Drainage capillary pressure data resulting from laboratory tests (solid symbols) and DRP (open symbols) for Rock Type 2. Colours correspond to cores.

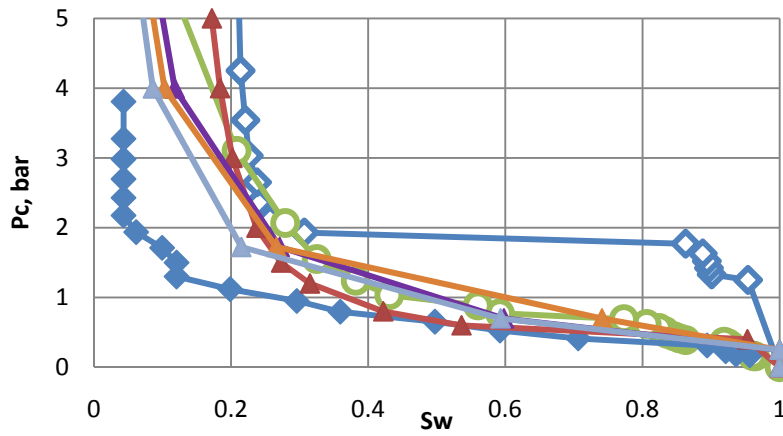


Figure 15. Drainage capillary pressure data resulting from laboratory tests (solid symbols) and DRP (open symbols) for Rock Type 4. Colours correspond to cores.